2017

A Chalcogenide Multimode Interferometric Temperature Sensor Operating at a Wavelength of 2 μm

Lin She

Pengfei Wang

Weimin Sun

See next page for additional authors

Authors

Lin She, Pengfei Wang, Weimin Sun, Xianfan Wang, Wenlei Yang, Gilberto Brambilla, and Gerald Farrell

A Chalcogenide Multimode Interferometric Temperature Sensor Operating at a Wavelength of 2 μm

Lin She, Pengfei Wang, Weimin Sun, Xianfan Wang, Wenlei Yang, Gilberto Brambilla, and Gerald Farrell

***Abstract*— This paper investigated the fabrication of a singlemode-multimode-singlemode fiber structure based on a chalcogenide (As_2S_3 and As_xS_{1-x}) multimode fiber sandwiched between two standard silica singlemode fibers using a commercial fiber fusion splicer. The temperature dependence of this hybrid fiber structure was investigated and a first proof of concept showed that the hybrid SMS fiber structure has an average experimental temperature sensitivity of circa 84.38 pm/°C over a temperature range of 20 °C∼100°C at the wavelength range around 2 μm. The measured results show a general agreement with numerical simulations based on a guided-mode propagation analysis method. Our result provides a potential platform for the development of compact, high-optical-quality, and robust sensing devices operating at the midinfrared wavelength range.**

***Index Terms*— Chalcogenide fiber, multimode interference, temperature sensor.**

I. Introduction

In RECENT years, multimode interference (MMI) effects have been intensively investigated in designing photonic integrated waveguides and the unique performance of self-imaging [1] of the input light field has been employed in a range of photonic devices, such as beam multiplexers combiners and splitters for applications in optical communications [2]–[4]. More recently MMI occurring in a singlemode–multimode–singlemode (SMS) fiber structures has been studied for applications in a range of sensing devices, e.g., displacement sensor [5], strain sensor [6], temperature sensor [7], refractometric sensor [8] and also as an edge filter for wavelength measurements [9].

Chalcogenides glasses are rapidly establishing themselves as technologically superior materials for emerging applications in non-volatile memory and high speed switching [10] and have been considered for a range of other optoelectronic technologies exploiting their extraordinary nonlinear optical properties. Chalcogenide fibers have been widely implemented in fiber evanescent spectroscopy experiments for detection of biochemical molecules in various applications, such as combustion gas detection [11], biochemical [12] and spectroscopy applications [13]. Also, recent research has shown that the mid-infrared signature of gases filling the holes of chalcogenide microstructured fiber can be easily detected [14]. To date, several applications, including ultrafast all-optical switching [15], supercontinuum generation [16], broadband wavelength conversion [17], all-optical signal processing [18] and Raman fiber lasers [19], have been demonstrated using chalcogenide glass fibers. Previously we have demonstrated a chalcogenide SMS fiber structure packaged in an UV epoxy and its multimode interference variation was observed as a result of photo-induced refractive index changes arising from either localized laser irradiation at a wavelength of 405 nm or through the use of a UV lamp [20]. In this work, to improve mechanical stability, a custom splicing method is used to replace the high precision translation stages and UV curable epoxy previously used for maintaining the mechanical alignment between the multimode fiber (MMF) and the singlemode fibers (SMFs). On the other hand, the diameter of the chalcogenide MMF previously employed was 275 μ m, much larger than that of the standard SMF. Therefore the mechanical stability of that SMS fiber structure was poor and also the alignment process was particularly challenging due the difference in fiber diameters between the silica SMFs and the chalcogenide MMF fixed by a UV curable epoxy.

In this paper, we present a customized chalcogenide fiber with a diameter of 125 μm based multimode interference device which was directly fabricated using a conventional fusion splicing method. Due to the large thermo-optical coefficient (TOC) and thermal expansion coefficient (TEC) of chalcogenide glass compared with silica, the temperature dependence of the transmission spectral response of this hybrid SMS structure is higher than that of conventional silica fiber based SMS devices, particularly at the mid-IR wavelength of

Manuscript received December 5, 2016; revised January 8, 2017; accepted January 8, 2017. Date of publication January 10, 2017; date of current version February 17, 2017. This work was supported in part by the 111 Project at the Harbin Engineering University under Grant B13015, in part by the National Natural Science Foundation of China (NSFC) under Grant 61575050, and in part by the Joint Research Fund in Astronomy through cooperative agreement between the National Natural NSFC and the Chinese Academy of Sciences (CAS) under Grant U1631239 and Grant U1331114. The work of G. Brambilla was supported by the Royal Society (London) for his research fellowship. The associate editor coordinating the review of this paper and approving it for publication was Prof. Tarikul Islam. *(Corresponding author: Pengfei Wang.)*

L. She, Weimin Sun, Xianfan Wang, and Wenlei Yang are with the Key Laboratory of In-Fiber Integrated Optics of Ministry of Education, College of Science, Harbin Engineering University, Harbin 150001, China (e-mail: lshe@hrbeu.edu.cn; sunweimin@hrbeu.edu.cn; heuwangfan@hrbeu.edu.cn; yangwenlei19851007@163.com).

P. Wang and G. Farrell are with the Key Laboratory of In-Fiber Integrated Optics of Ministry of Education, College of Science, Harbin Engineering University, Harbin 150001, China, and also with the Photonics Research Centre, Dublin Institute of Technology, 8 Dublin, Ireland (e-mail: pengfei.wang@dit.ie; gerald.farrell@dit.ie).

G. Brambilla is with the Optoelectronics Research Centre, University of Southampton, Southampton SO17 1BJ, U.K. (e-mail: gb2@orc.soton.ac.uk).

Digital Object Identifier 10.1109/JSEN.2017.2651382

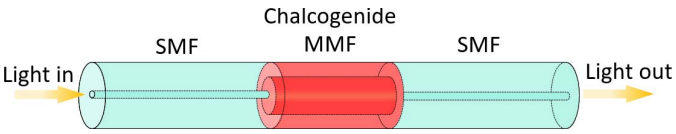

Fig. 1. Schematic of an SMS fiber structure based on silica singlemode fiber-chalcogenide multimode fiber-silica singlemode fiber.

$\lambda = 2\ \mu$m. The fabricated device offers the potential for low-cost, robustly assembled fully integrated sensing devices for the measurement of temperature or refractive index over the near- and mid-infrared wavelength ranges, and also provides a promising platform for developing a range of nonlinear fiber devices with non-linearity thresholds orders of magnitudes lower by comparisonto conventional all-silica based fiber devices.

An SMS fiber structure consists of input and output silica singlemode fibers (SMFs) with a short section of multimode fiber (MMF) sandwiched between them as shown in Fig. 1. While multimode interferometers usually employ silica MMFs, in this paper a chalcogenide MMF section was sandwiched between two standard silica singlemode fibers.

II. Theoretical Analysis

The input field provided by the SMF can be approximated as a Gaussian beam with a field distribution of *E(r,0)* because of the symmetric cylindrical characteristic of fundamental mode of the input SMF. Traditionally the input Gaussian beam can excite a specific number of guided high-order modes in the MMF, namely, the input field can be decomposed by the eigenmodes of linearly polarized (LP) mode of LP_{nm}. However in fact only the LP_{0m} modes can be effectively excited due to the circular symmetry of the input field and assuming an ideal alignment of the central axes of the fibers cores of the SMF and MMF. The details regarding this theoretical analysis have been addressed in [21].

In order to gain a better insight into the operation of the device, the SMS spectral properties were simulated using a conventional cylindrical wide-angle beam propagation method presented in [22]. As well-known, the wave-equation for the light propagating in an MMF is

$$\frac{\partial^2 E}{\partial r^2} + \frac{1}{r}\frac{\partial E}{\partial r} + \frac{\partial^2 E}{\partial z^2} + k^2 n^2 E = 0 \tag{1}$$

where $k = 2\pi/\lambda$ and λ is the wavelength in free-space. Here a slowly varying envelope approximation involves replacing the quickly varying component with a slowly varying function is used to solve the above wave-equation, i.e., $E(r,z) = \hat{E}(r,z)\exp(jkn_0 z)$ (where n_0 is reference refractive index and $j = \sqrt{-1}$). For $\hat{E}(r,z)$, the beam propagation equation can be written as follows:

$$\frac{\partial \hat{E}}{\partial z} = \frac{\frac{j}{2kn_0} P\hat{E}}{1 - \frac{j}{2kn_0}\frac{\partial \hat{E}}{\partial z}} \tag{2}$$

where $P\hat{E} = \left[\frac{\partial^2 \hat{E}}{\partial r^2} + \frac{1}{r}\frac{\partial \hat{E}}{\partial r} + k^2\left(n^2(r,z) - n_0^2\right)\hat{E}\right]$. Considering a number of approximation and numerical calculation methods, such as the Padé approximation, Crank-Nicholson finite-difference scheme and multi-step method, the above

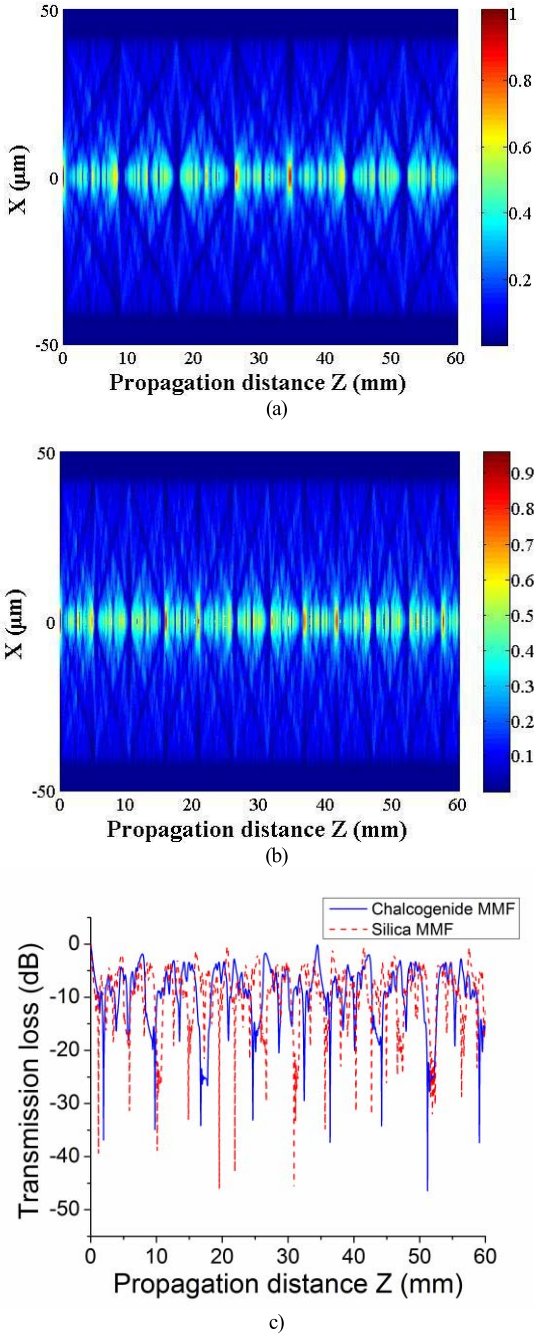

Fig. 2. (a) Intensity distribution within the chalcogenide multimode fiber section of the SMS structure. (b) Intensity distribution within a silica multimode fiber section of the SMS structure. (c) Calculated transmissivity to the output singlemode fiber for different chalcogenide & silica multimode fiber lengths when the operating wavelength is $\lambda = 2\ \mu$m.

Eq.(1) can be solved iteratively, namely, for the i-th step, we have

$$\begin{aligned} &a_i^* \eta_- \hat{E}_{m-1}^{l+\frac{i}{n}} + \left[1 + a_i^* \varsigma\right] \hat{E}_m^{l+\frac{i}{n}} + a_i^* \eta_+ \hat{E}_{m+1}^{l+\frac{i}{n}} \\ &\quad = a_i \eta_- \hat{E}_{m-1}^{l+\frac{i-1}{n}} + \left[1 + a_i \varsigma\right] \hat{E}_{m-1}^{l+\frac{i-1}{n}} + a_i \eta_+ \hat{E}_{m+1}^{l+\frac{i-1}{n}} \end{aligned} \tag{3}$$

where $\eta_\pm = \frac{1}{\Delta r^2} \pm \frac{1}{2r\Delta r}$ and $\varsigma = \left(k^2\left(n^2 - n_0^2\right) - \frac{2}{\Delta r^2}\right)$. a_i and $a_i^* (i = 1, 2, \ldots n)$ are determined by the polynomials based on the Padé approximation. At the fiber axis, $r = 0$, therefore L' Hospital's rule is used and the corresponding

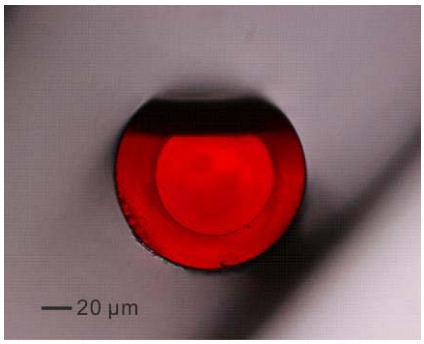

Fig. 3. Microscope image of chalcogenide multimode fiber cross section.

Fig. 4. Image of a chalcogenide multimode fiber with a length of circa 24.75 mm spliced with a silica singlemode fiber.

equation can be written as:

$$\left[1+a_i^*\left(k^2\left(n^2-n_0^2\right)-\frac{4}{\Delta r^2}\right)\right]E_0^{l+\frac{i}{n}}+a_i^*\frac{4}{\Delta r^2}E_1^{l+\frac{i}{n}} =\left[1+a_i\left(k^2\left(n^2-n_0^2\right)-\frac{4}{\Delta r^2}\right)\right]E_0^{l+\frac{i-1}{n}} +a_i\left[\frac{4}{\Delta r^2}\right]E_1^{l+\frac{i-1}{n}} \quad (4)$$

Here in the theoretical model, only the half-plane of the proposed SMS structure, i.e. $0 \le r \le R$ is used as the calculation window and as usual the perfectly matched layer is adopted at the boundary of the calculation area ($r = R$) based on the symmetric cylindrical coordinate system of the proposed SMF fiber structure,

To calculate the transmission loss of the SMS fiber structure, the overlap integral is used as follows:

$$T_s(l)=10\log_{10}\left(\frac{\left|\int_{-\infty}^{\infty}E(l,r)\,F(r)\,dr\right|^2}{\int_{-\infty}^{\infty}|E(l,r)|^2\,dr\int_{-\infty}^{\infty}|F(r)|^2\,dr}\right) \quad (5)$$

where l is the length of multimode fiber section, $E(l,r)$ is the calculated field at the interface between the MMF section and the output SMF and $F(r)$ is the eigenmode of the output SMF.

The intensity distribution of the propagation field and the transmissivity of the SMS structure was calculated using the above WA-BPM and are presented in Fig. 2. From the simulation results presented in Fig. 2a, one can see that the light converges periodically while propagating in the chalcogenide MMF section. The first convergence occurs around the length of 10 mm due to the maximal interference between different modes of the multimode fibre. However for Fig. 2b, the first significant convergence occurs about the length of 5 mm of the silica MMF section. To better characterize the difference between the two MMFs, the transmissivities of both

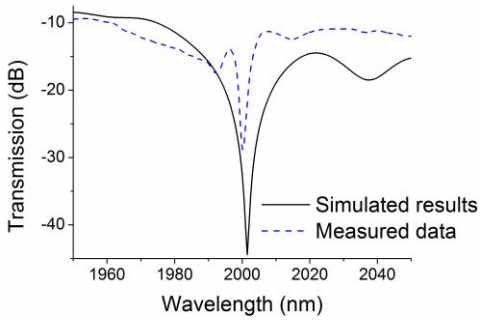

Fig. 5. Calculated (black line) and measured (blue dashed line) spectral response of the hybrid silica-chalcogenide SMS device over a wavelength range of 1950∼2050 nm.

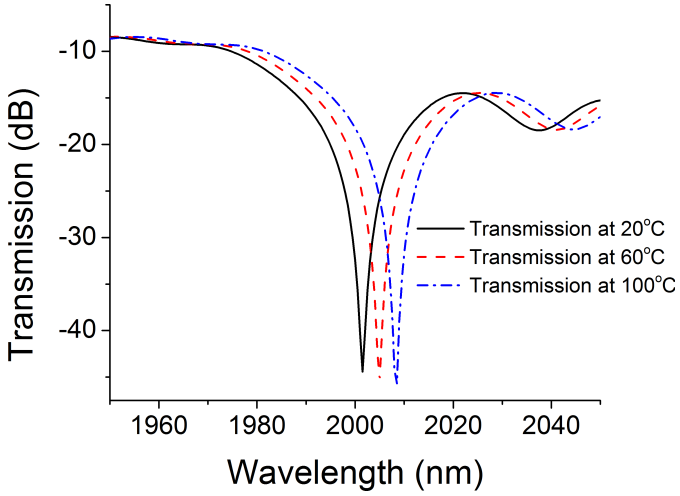

Fig. 6. Calculated spectral responses of the hybrid silica-chalcogenide SMS device over a wavelength range of 1950∼2050 nm at room temperature (20 °C, dark line), 60 °C (red dashed line), 100 °C (blue dashed dot line).

SMS structures were calculated based on the Equation (5), the calculated results are presented in Figure 2c. Figure 2c shows that the transmissivity of the chalcogenide MMF (blue solid line) reaches a maximum value of -46.45 dB at a propagation position of z = 51.2 mm at $\lambda = 2$ μm. Compared with the calculated results of silica MMF (red dashed line), the calculated results of chalcogenide MMF show that the eigenmode interference within the MMF section is determined by both the size and the refractive index of the As_2S_3 MMF core. In terms of all the modelled results, for chalcogenide MMF, the input light is re-imaged at a propagation distance 34.46 mm from the input fiber with a transmissivity of -0.1601 dB along the chalcogenide MMF, which is significantly different from the results of the silica SMS fiber device with multiple re-imaging positions at 20.78 mm, 41.55 mm and 57.52 mm.

III. Experimental Investigation and Discussion

The chalcogenide fiber used in the experiments was a step-index multimode fiber with an As_2S_3 core (diameter is 82 μm) and As_xS_{1-x} ($0.15 \le x \le 0.43$) cladding (diameter is 125 μm). The refractive index of the core and the cladding of the input/output SMF is 1.4438 and 1.4381 and the refractive index of the core and the cladding of chalcogenide MMF is 2.4261 and 2.4087 at the wavelength of 2 μm, respectively.

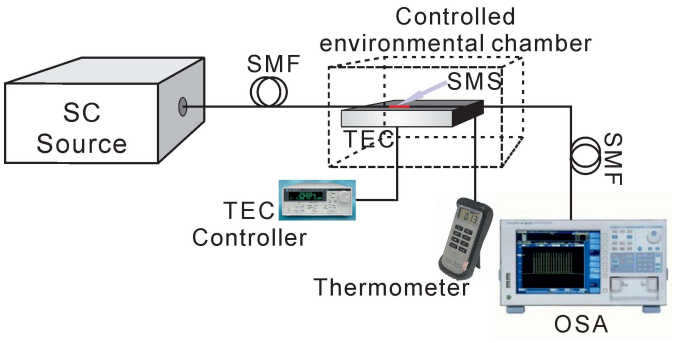

Fig. 7. Experimental setup for the temperature measurements of the hybrid SMS fiber structure.

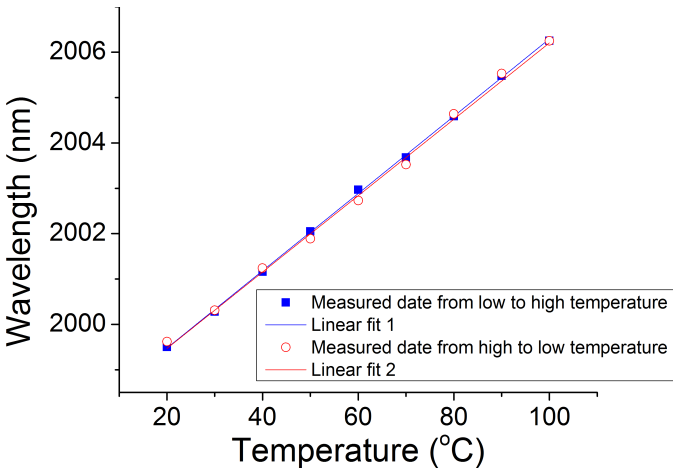

Fig. 8. Dip wavelength as a function of temperature. The blue squares represent the measured data from low to high temperature, the red circles the measured data from high to low; blue and red lines represent the linear fits, respectively.

The chalcogenide multimode fiber cross section is shown in Fig 3.

The SMS sample was manufactured by sandwiching the chalcogenide multimode fiber between two silica SMFs and fusing the joints using a high precision Ericsson manual control fusion splicer (FSU-995PM). Fig. 4 shows the resulting hybrid SMS structure manufactured from a 24.75 mm long chalcogenide multimode fiber spliced with a silica singlemode fiber. A transmission spectra for the fabricated hybrid SMS fiber device were recorded using a supercontinuum light source (450∼2100 nm) and an optical spectrum analyzer (YOKOGAWA AQ6375).

Figure 5 presents the calculated and measured transmission spectra of the hybrid silica-chalcogenide SMS structure over a wavelength range of 1950-2050 nm, where the chalcogenide MMF length is circa 24.75 mm. The measured results show a general agreement with theoretical predictions. The discrepancy between the calculated and measured results could be due to the central alignment between the silica SMFs and the chalcogenide MMF, the deformation of the chalcogenide MMF over the splicing joint induced by arc heating, the length control of the chalcogenide MMF and the approximations made in the calculation (simulated transmission for an SMS includes some approximations in the WA-BPM mode, such as assuming only LP_{0m} fundamental modes were excited in the theoretical model, slowly varying envelope approximation and Padé approximation).

It is well-known that chalcogenide glasses have a lower working temperature (from 300 °C to 400 °C, e.g. As_2S_3 has a working temperature of 310 °C), a larger thermo-optic coefficient (TOC) of circa 5×10^{-5}/°C and thermal expansion coefficient (TEC) of 2.14×10^{-5}/°C, compared with those of conventional fused silica material. Based on the WA-BPM model in a symmetric cylindrical coordinate system consisting of the TOC and TEC effects of each fiber layer [23], the transmission of the silica-chalcogenide-silica SMS structure was simulated and is presented in Fig. 6. The calculated transmission responses of the hybrid SMS fiber over a wavelength range from 1950 nm to 2050 nm for three temperatures, T = 20°C, 60°C and 100°C, are plotted in Fig. 6, which are based on simulations of light propagating through the whole length of 24.75 mm hybrid SMS fiber structure.

From Fig. 6, it is clear that the dip wavelength redshifts to longer wavelengths when the surrounding temperature increases which is expected given both the TOC and TEC of the chalcogenide material. The average simulated temperature sensitivity over the temperature range from 20°C to 100°C was circa 87.5 pm/°C which is one order of magnitude higher than 8.7 pm/°C, recorded in the silica SMS structure reported by Wu *et al.* in [24]. This behavior indicates that temperature-induced variations in the transmission response of the multimode interferences within the chalcogenide MMF are strongly influenced by the surrounding environment and such a temperature dependence can be used for a high sensitivity temperature sensing applications over a mid-infrared wavelength range. Also, the temperature sensitivity of the proposed hybrid SMS fiber structure can be affected by the length and the core diameter of the chalcogenide fiber, and by the sensing scheme used in the measurements. Further work to improve the temperature sensitivity is under way.

To experimentally study the temperature dependence of the hybrid SMS fiber structure, the sample was placed on a thermoelectric cooler (TEC) as shown in Fig. 7. The temperature of the TEC element was controlled by a temperature controller. A thermistor was used to provide temperature feedback to the controller from the TEC element. An additional handheld thermometer was used to confirm the temperature changes on the TEC surface. The entire setup was placed inside a small controlled environmental chamber. For the purpose of this experiment the ambient temperature inside the chamber was fixed at 20° C (room temperature) as a starting point. A supercontinuum source was used for launching power into the SMS device and the wavelength shifts was monitored by an optical spectrum analyzer.

To determine the temperature dependence of the device the interference peak shift was observed while varying the temperature of the device from 20° C to 100° C. Fig. 8 shows the measured temperature dependence for the hybrid SMS device over a temperature range from 20 °C to 100 °C. When the temperature is increased from 20° C to 100° C in intervals of 10°C the interference peak exhibits minute shifts to longer wavelengths. Both data sets show a good linearity, demonstrated by a linear regression value of R2 = 0.9998

and 0.9986, respectively. As expected the measured thermal sensitivity of the SMS device is reasonable high, confirmed by the thermal sensitivity obtained in the experiment for the hybrid SMS device which is circa 84.38 pm/° C. The measured results have a good agreement with the theoretical prediction of 87.5 pm/° C. Overall, the temperature sensitivity measured in our work is higher than the experimental results presented in [24].

IV. Conclusion

In conclusion, as a first proof of concept, we have proposed and demonstrated a chalcogenide MMF based hybrid SMS structure using a conventional fusion slicing method. The experimental characterization showed a good agreement with numerical simulations. Due to the high TOC and TEC of the chalcogenide glass material itself, the chalcogenide SMS fiber structure has a high measured temperature sensitivity of 84.38 pm/° C which is higher than that of a silica fiber based SMS device. Also thanks to the ultra-broad transmission window of the chalcogenide glass itself, this hybrid SMS fiber structure can be further developed to sense a range of physical parameters, such as temperature, refractive index and strain over near- and mid-IR wavelength ranges if we replace the silica SMFs to chalcogenide SMFs. This geometry may also become a promising platform for developing a range of nonlinear fiber devices with thresholds orders of magnitudes lower compared to conventional silica based fiber devices. Corresponding research on this topic is underway.

References

[1] L. B. Soldano and E. C. M. Pennings, "Optical multi-mode interference devices based on self-imaging: Principles and applications," *J. Lightw. Technol.*, vol. 13, no. 4, pp. 615–627, Apr. 1995.

[2] W. Chen *et al.*, "Electro-optical logic gates based on graphene-silicon waveguides," *Opt. Commun.*, vol. 372, pp. 85–90, Aug. 2016.

[3] L. Han, S. Liang, J. Xu, L. Qiao, H. Zhu, and W. Wang, "Simultaneous wavelength- and mode-division (De)multiplexing for high-capacity on-chip data transmission link," *IEEE Photon. J.*, vol. 8, no. 2, pp. 1–10, Feb. 2016.

[4] A. Zanzi, A. Brimont, A. Griol, P. Sanchis, and J. Marti, "Compact and low-loss asymmetrical multimode interference splitter for power monitoring applications," *Opt. Lett.*, vol. 41, no. 2, pp. 227–229, 2016.

[5] Q. Wu, Y. Semenova, A. Hatta, and G. Farrell, "Experimental demonstration of a simple displacement sensor based on a bent singlemode-multimode-singlemode (SMS) fiber structure," *Meas. Sci. Technol.*, vol. 22, no. 2, p. 025203, 2011.

[6] L. Ma, Y. Qi, Z. Kang, and S. Jian, "All-fiber strain and curvature sensor based on no-core fiber," *IEEE Sensors J.*, vol. 14, no. 5, pp. 1514–1517, May 2014.

[7] Y. Zhao, P. Wang, R. Lv, and Y. Yang, "Temperature sensing characteristics based on up-taper and single mode–multimode fiber structure," *IEEE Photon. Technol. Lett.*, vol. 28, no. 22, pp. 2557–2560, Nov. 15, 2016.

[8] Y. Chen *et al.*, "A hybrid multimode interference structure-based refractive index and temperature fiber sensor," *IEEE Sensors J.*, vol. 16, no. 2, pp. 331–335, Feb. 2016.

[9] A. M. Hatta, G. Farrell, Q. Wang, G. Rajan, P. Wang, and Y. Semenova, "Ratiometric wavelength monitor based on singlemode-multimode-singlemode fiber structure," *Microw. Opt. Technol. Lett.*, vol. 50, no. 12, pp. 3036–3039, Dec. 2008.

[10] B. J. Eggleton, B. Luther-Davies, and K. Richardson, "Chalcogenide photonics," *Nature Photon.*, vol. 5, no. 3, pp. 141–148, 2011.

[11] X. Dai *et al.*, "A novel image-guided FT-IR sensor using chalcogenide glass optical fibers for the detection of combustion gases," *Sens. Actuators B, Chem.*, vol. 220, pp. 414–419, Sep. 2015.

[12] P. Lucas and B. Bureau, "Selenide glass fibers for biochemical infrared sensing," in *Applications of Chalcogenides: S, Se, and Te*. Berlin, Germany: Springer, 2017, pp. 285–319.

[13] R. Chahal *et al.*, "Fiber evanescent wave spectroscopy based on IR fluorescent chalcogenide fibers," *Sens. Actuators B, Chem.*, vol. 229, pp. 209–216, Oct. 2016.

[14] F. Charpentier *et al.*, "CO_2 detection using microstructured chalcogenide fibers," *Sensor Lett.*, vol. 7, no. 5, pp. 745–749, 2009.

[15] J. M. Harbold, F. O. Ilday, F. W. Wise, and B. G. Aitken, "Highly nonlinear Ge-As-Se and Ge-As-S-Se glasses for all-optical switching," *IEEE Photon. Technol. Lett.*, vol. 14, no. 6, pp. 822–824, Jun. 2002.

[16] Y. Yu *et al.*, "1.8-10 μm mid-infrared supercontinuum generated in a step-index chalcogenide fiber using low peak pump power," *Opt. Lett.*, vol. 40, no. 6, pp. 1081–1084, 2015.

[17] A. Pelé *et al.*, "Wavelength conversion in Er 3+ doped chalcogenide fibers for optical gas sensors," *Opt. Exp.*, vol. 23, no. 4, pp. 4163–4172, 2015.

[18] E. Yousefi, M. Hatami, and A. T. Jahromi, "All-optical ternary signal processing using uniform nonlinear chalcogenide fiber Bragg gratings," *J. Opt. Soc. Amer. B*, vol. 32, no. 7, pp. 1471–1478, 2015.

[19] M. Bernier *et al.*, "3.77 μm fiber laser based on cascaded Raman gain in a chalcogenide glass fiber," *Opt. Lett.*, vol. 39, no. 7, pp. 2052–2055, 2014.

[20] P. Wang, M. Ding, L. Bo, Y. Semenova, Q. Wu, and G. Farrell, "A silica singmode fibre-chalcogenide multimode fibre-silica singlemode fibre structure," *Photon. Lett. Poland*, vol. 4, no. 4, pp. 143–145, 2012.

[21] W. S. Mohammed, A. Mehta, and E. G. Johnson, "Wavelength tunable fiber lens based on multimode interference," *J. Lightw. Technol.*, vol. 22, no. 2, pp. 469–477, Feb. 2004.

[22] Q. Wang and G. Farrell, "All-fiber multimode-interference-based refractometer sensor: Proposal and design," *Opt. Lett.*, vol. 31, no. 2006, pp. 317–319.

[23] P. Wang, Y. Semenova, and G. Farrell, "Temperature dependence of macrobending loss in all-fiber bend loss edge filter," *Opt. Commun.*, vol. 281, no. 17, pp. 4312–4316, 2008.

[24] Q. Wu *et al.*, "Bent SMS fibre structure for temperature measurement," *Electron. Lett.*, vol. 46, no. 16, pp. 1129–1130, 2010.

Lin She received the B.S. degree in optical fiber communications from Jilin University in 1999. She is currently pursuing the Ph.D. degree in optical engineering with Harbin Engineering University, Harbin China. Her research interests include mid-IR fibers-based photonic devices.

Pengfei Wang received the Ph.D. degree of optics engineering from the Photonics Research Centre, Dublin Institute of Technology (DIT), Dublin, Ireland, in 2008. He was with the European Space Agency and the Italian Space Agency, Institute of Microelectronics and Microsystems, Italian National Research Council, Bologna, Italy, sponsored by both the Italian Ministry of Foreign Affairs and the United Nations Educational, Scientific and Cultural Organization, as a Research Assistant, from 2004 to 2005. He was a Research Associate with the Photonics Research Centre, DIT, supported by the Irish Research Council Government Postdoctoral Scholarship from 2009 to 2010. In 2010, he joined the Optoelectronics Research Centre, University of Southampton, funded by the EU Marie Curie Research Fellowship. In 2011, he joined the Advanced Laser Laboratory of SPI Lasers, Southampton, as a part-time Research Fellow. He was appointed a Senior Research Fellow (Tenured) with the PRC, DIT, from 2013 to 2015. Since 2015, he has been with the College of Science, Harbin Engineering University, China, as a full-time Distinguished Professor, sponsored by the Chinese government Program entitled The Recruitment Program of Global Youth Experts. He has authored and co-authored over 160 papers in academic journals and international conferences so far. His research interests include compound glass materials, fiber lasers, computational photonics, including modeling, simulation and optimization, photonic devices, such as microfiber/nanowire based photonic devices, fiber optic sensors, photonic integrated circuits, liquid crystal-based photonic devices, laser micromachining, and applications development, including optical communication and optical sensing.

Weimin Sun received the B.S. degree from Peking University, China, in 1990, the M.S. degree from the Harbin Institute of Technology, China, in 1993, and the Ph.D. degree from Harbin Engineering University, China, in 2005. In 1995, he joined Harbin Engineering University, where he is currently a Professor and the Executive Dean of the Undergraduate College. He is the Vice-Chairman of the Physical Society and the Vice-Chairman of the Optical Society, Heilongjiang, China. He has authored and coauthored over 200 journal and conference papers and 15 patents. His research interests include astrophotonics, biophotonics, fiber integrated components, and optical sensors.

Xianfan Wang received the Ph.D. degree in photonics from Harbin Engineering University in 2016. She currently holds the post-doctoral position with the Key Lab of In-fiber Integrated Optics, Ministry Education of China, Harbin Engineering University, China. Her research interests include fiber-optic sensing and long period fiber grating.

Wenlei Yang received the Ph.D. degree in photonics from Harbin Engineering University, China, in 2016. She currently holds a post-doctoral position with the Key Lab of In-Fiber Integrated Optics, Ministry Education of China, Harbin Engineering University, China. Her research interests include fiber-optic sensing and long period fiber grating.

Gilberto Brambilla received the Ph. D. degree in photonics from Harbin Engineering University, China, in 2016. She is currently working toward the post-doctoral position at the Key Lab of In-fiber Integrated Optics, Ministry Education of China, Harbin Engineering University, China. Her research interests include fiber-optic sensing and long period fiber grating.

Gerald Farrell received the electronic engineering degree from the University College Dublin in 1979 and the Ph.D. degree from the Trinity College Dublin for research in all-optical synchronization using self-pulsating laser diodes. He spent a number of years as a design engineer developing optical fiber transmission systems before joining the Dublin Institute of Technology (DIT). Between 1997 and 2003, he was a Director of the startup company PX Instrument Technology, focusing on optical fiber system test and measurement systems. Prof. Farrell is the Founder and Director of the DIT Photonics Research Centre. He leads a multinational research team of doctoral, postdoctoral, and senior researchers focusing on several areas of optical fiber sensing research including photonic crystal fiber sensors for environmental and energy systems sensing, novel sensors for composite materials and medical devices, LC infiltrated PCF sensors, and micro-fiber and nanowire sensors for chemical and biosensing. He has also led the development of research collaborations with a number of research groups in China, Poland, and elsewhere. He has over 320 publications in the area of photonics. He is a member of the Optical Society of America and an Advisory Professor with the Beijing University of Posts and Telecommunications, China, and Harbin Engineering University. He is also Dean of the College of Engineering and Built Environment, DIT.